Mon. Not. R. Astron. Soc. **000**, 1–7 (2011) Printed 12 September 2012 (MN LATEX style file v2.2)

Determining neutron star masses with weak microlensing

Lanlan Tian[1] and Shude Mao[1,2]
[1] *National Astronomical Observatories, Chinese Academy of Sciences, Beijing, 100012, China*
[2] *Jodrell Bank Centre for Astrophysics, The University of Manchester, Alan Turing Building, Manchester M13 9PL, UK*

Accepted ..... Received ..... ; in original form.....

ABSTRACT
The masses of stars including stellar remnants are almost exclusively known from binary systems. In this work, we study gravitational microlensing of faint background galaxies by isolated neutron stars (pulsars). We show that the resulting surface brightness distortions can be used to determine the masses of neutron star. Due to different evolutionary histories, isolated neutron stars may have different masses from those in binary systems, and thus provide unique insight into their equation of states under extreme physical conditions. We search for existing pulsar catalogues and find one promising pair of a nearby pulsar and a background galaxy. This method will become more practical for the next generation optical and radio surveys and telescopes.

Key words: Gravitational lensing: micro - stars: neutron - stars: pulsars

1 INTRODUCTION

From stellar evolution, numerous ($\sim 10^8$) neutron stars are expected in the Galaxy (e.g. Arzoumanian et al. 2002). So far only a tiny fraction of these have been discovered, mostly as pulsars. Even a small fraction have measured masses, usually for binary systems (due to additional orbital information). However, the masses of these neutron stars may well be affected by physical processes (e.g. accretion) between the companions. The masses of isolated stellar remnants (such as neutron stars) are thus of particular interests since they may be more easily compared to that predicted by stellar evolution; such comparison can provide important constraints on the equation of state under extreme physical (e.g. density) conditions.

The recent discovery of a $2M_\odot$ neutron star in a binary system already rules out some equation of state (Demorest et al. 2010). More mass determinations of neutron stars in isolated or binary systems would be important for such constraints. Gravitational microlensing has already demonstrated its capabilities to measure the masses of isolated normal stars (see, e.g., Smith et al. 2003; Gould et al. 2009; Hwang et al. 2010; Batista et al. 2009; see Mao 2012 for a review).

Paczynski (1995) studied how the masses of nearby dwarfs with high proper motions can be determined using microlensing, while Coles et al. (2010) studied how "weak" microlensing of background galaxies can be used to determine the masses of nearby stars. For the usual "strong" microlensing, we observe the magnification change as a function of time; in "weak" microlensing, we observe the surface brightness distortions of the background galaxy by the nearby lens as it moves across the galaxy. The Coles et al. (2010) study has one potential difficulty, that is, their nearby stars will be very bright compared to the background galaxy, and so some type of coronagraph has to be used to block the light from the foreground star. In this work, we study gravitational microlensing of background galaxies by nearby stellar remnants ($\lesssim$ 1kpc). The stellar remnants are expected to be faint in the optical, and so the "glaring" problem will be much less severe.

The outline of this paper is as follows. In §2 we first briefly recall the method of Coles et al. (2010). In §3, we perform simulations for the Thirty Meter Telescope (TMT[1]). In §4 we perform a preliminary search for pulsars overlap with background galaxies, and present some preliminary matches. In §5 we discuss our results further.

2 METHOD

In principle if we have an image of the background galaxy at the time before the lens star crosses in front of the galaxy and a second image when the lens star is passing the galaxy, a simple subtraction of the two images will reveal the distortions by the lens. From these distortions, we can derive the angular position of the lens star and the corresponding Einstein radius. If the lens distance is known, then the mass of the lens star can be directly estimated from the derived Einstein radius by

[1] www.tmt.org

$$\theta_E \approx 0.09'' \sqrt{\frac{M/M_\odot}{D_{\rm L}/{\rm pc}}}, \quad (1)$$

where $D_{\rm L}$ is the distance to the lens, M is the lens mass, and we have assumed the source is much further away from us than the lens. In practice, the procedure requires the Einstein radius to be sufficiently large and the signal-to-noise ratio sufficiently high.

From the presently known catalogues of neutron stars and pulsars (see section 4), it appears rare that a galaxy is located in the vicinity of a pulsar or a neutron star. For example, in our search results, the smallest angular separation between seven ROSAT discovered isolated neutron stars and the background galaxies is $\sim 50''$. Although these stars are nearby and have relatively high proper motions (hundreds of milli-arcsecs per year), such a separation will still require a neutron star more than fifty years to overlap with the background galaxy even if it moves in the right direction.

We explore an alternative if we have only one image of the background galaxy when the foreground star is already well aligned with the background object. If the (unlensed) surface brightness of the background galaxy is smooth on the scale of the lens distortions ($\sim 0.1''$), it is plausible that the observed distortions are due to the lens, from which we can derive the Einstein radius of the lens star (see Coles et al. 2010). In practice, we may have two images where the lens moved a detectable distance within a few years, which will allow a difference image to be obtained; we return to this point in the discussion.

Let us consider an unlensed image S of the background galaxy. It can be expanded in terms of basis functions $B^n(\vec{\theta})$ as

$$S = \sum_n a^n B^n(\vec{\theta}), \quad (2)$$

where a^n's are the expansion coefficients. Since lensing conserves surface brightness, the lensed image of the galaxy is

$$D = \sum_n a^n B^n(\vec{\phi}(\vec{\theta}, \vec{z_t}, \theta_E)), \quad (3)$$

where $\vec{z_t}$ is the position of the lens star and the point $\vec{\phi}$ in the source is given by the lens equation:

$$\vec{\phi} = \vec{\theta} - \theta_E^2 \frac{\vec{\theta} - \vec{z_t}}{|\vec{\theta} - \vec{z_t}|^2}. \quad (4)$$

Now we have a model of the lensed image D. Assuming the lens position is precisely known, we have one parameter θ_E, which we would like to determine, and a set of parameters a^n's, which are not of interests. Once we have an observed lensed image d_{ij} at t when the lens star has a position $\vec{z_t}$, the maximum likelihood is given by

$$L(a^n, \theta_E) = \prod_{ij} \exp[-\frac{1}{2}\sigma_{ij}^{-2}(d_{ij} - D_{ij})^2], \quad (5)$$

where σ_{ij} is the noise, ij runs the pixel. We assume the measurement errors are Gaussian. Because of this assumption and the fact that the model D is a linear function of the expansion coefficients a^n, we can marginalise the coefficients a^n and only leave one parameter θ_E in the marginalised likelihood (see eq. 8 in Coles et al. 2010). For clarity, we rewrite the marginalised likelihood as:

$$\chi^2 = 2\ln L(\theta_E) = \ln|\det C| + \sum_{mn} P_m P_n C_{mn} - \sum_{ij} \sigma_{ij}^{-2} d_{ij}^2, \quad (6)$$

where

$$P_n = \sum_{ij} \sigma_{ij}^{-2} d_{ij} L_{ij}^n \quad (7)$$

and

$$C_{mn}^{-1} = \sum_{ij} \sigma_{ij}^{-2} L_{ij}^m L_{ij}^n. \quad (8)$$

The Einstein radius θ_E is involved in the terms L_{ij}^n through

$$L_{ij}^n = B^n(\vec{\phi}(\vec{\theta}_{ij}, \vec{z_t}, \theta_E)), \quad (9)$$

which are the "lensed" basis functions. Once the noise level σ_{ij} is given from the observed lensed image d_{ij}, we can obtain the best-fit Einstein radius θ_E by minimising the χ^2.

With this method, even though we do not know the unlensed image, we can still derive the Einstein radius θ_E from one observed lensed image. There is, however, an underlying assumption that the distortion around the lens is not due to any "substructure" in the background galaxy.

3 SIMULATIONS

In the section, we explore the feasibility of deriving the Einstein radii of the pulsars or isolated neutron stars and study the corresponding errors.

First, we produce a simulated lensed image of the background galaxy. We assume the unlensed surface brightness follows a de Vaucouleurs (1948) profile. We would like to stress that the specific form of the unlensed image of the galaxy is not important as long as it is smooth on a scale a few times the Einstein radius of the lens star. In practice, it remains to be seen whether this condition is satisfied in real images.

The pair search in Section 4 suggests that the background source will be faint and the photons from the sky background dominate the noise. Here we consider a specific example. We assume the source galaxy has a magnitude $J = 19.86$ and the sky surface brightness is $J = 16.75\,{\rm mag}/''^2$, appropriate for the darkest nights on Mauna Kea (Sánchez et al. 2008). It turns out that in the region we consider ($0.284'' \times 0.284''$) the flux from the sky background is 12.5 times that from the source galaxy. So in our simulation, the noise comes from two parts: one from the source itself and one from the sky background. Both follow the Poisson distribution. We then obtained the simulated lensed image at each pixel d_{ij} from this Poisson distribution. The mean of the Poisson distribution is the corresponding lensed brightness S_{ij} (converted into photon counts) plus photons from the sky background. The lensed brightness S_{ij} is given by

$$S_{ij}(\theta_{ij}) = \exp(-7.67[\sqrt{(\phi_{ij}/R_e)^2 + R_c^2}]^{1/4}) \quad (10)$$

with an effective radius $R_{\rm e} = 1''$ and a core radius $R_{\rm c}$ of 2 pixels (which mimics seeing). The connection between θ_{ij} and ϕ_{ij} in Eq. (10) is given by Eq. (4). The noise σ_{ij} is taken as $\sqrt{d_{ij}}$.

We specialise to the case for the next-generation extremely large optical-IR telescopes, in particular the TMT.

For the first-light instrument, the InfraRed Imaging Spectrograph (IRIS), the pixel size is $0.004''$ and the diffraction-limited resolution is $0.007''$ at 1 micron. In our simulation, we use the IRIS pixel size as the minimum scale in the choice of the scale parameter β in the basis functions (see below).

We assume the lenses are nearby stars in the Milky Way and the background galaxies are far away. For the known closest isolated neutron star, the measured distance is about 160 pc (Posselt et al. 2009), if we assume its mass is $1.4M_{\odot}$, then $\theta_E \approx 0.008''$. For the pulsar (J1238+21) which is crossing in front of a galaxy right now, using a mass of $1.4M_{\odot}$ and the estimated distance 1.7 kpc, we obtain $\theta_E \approx 0.0025''$. Considering TMT has a resolution of $0.007''$, we take $\theta_E = 0.005''$ and $\theta_E = 0.01''$ in our simulations to produce the lensed images.

We use shapelets as the basis functions. As we know, a faithful shapelets decomposition depends on four parameters: the scale parameter β, the maximum order of shapelets order $N_{\max}$ and the choice of the centroid position of the galaxy (Melchior et al. 2007). The minimum and maximum sizes of features that can be resolved by the shapelets are respectively (Refregier 2003) $\theta_{\min} \approx \beta(n_{\rm total}+1)^{-1/2}, \theta_{\max} \approx \beta(n_{\rm total}+1)^{1/2}$, where $n_{\rm total}$ is the sum of the maximum orders for two dimensions ($N_{x,\max}$ and $N_{y,\max}$).

In our tests, we find the scale parameter β affects the χ^2 fitting the most. An arbitrary choice of β can cause a mis-estimation of the coefficients a_n. Since the set of a_n represents the unlensed image, a mis-estimation of a_n can lead to a mis-representation of the unlensed image. Although a_n's are marginalised out, our tests show the different choices of β can still affect the behaviour of the effective χ^2. Therefore, it is necessary to find an optimal β in advance. In our tests, we found the value of optimal β changes with the size of the pixel and the Einstein radius. In this simulation, we use the pixel size of $0.004''$, and $\theta_E = 0.005''$. The maximum order of the basis function is set to $N_{\max} = 21$ for both two dimensions (x and y). The centre of the image is fixed at the centre of the grid box. Refregier (2003) suggested that for a given $\theta_{\min}$ and $\theta_{\max}$ a good choice for β is $\approx (\theta_{\min}\theta_{\max})^{1/2}$. Following this, we choose the minimum scale as the pixel size ($0.004''$) and the maximum scale as the box size ($0.284''$), and the final chosen scale parameter is $\beta = 0.03''$.

When the Einstein radius is as small as $0.005''$, the area affected by lensing is small (if we consider 20 times the Einstein radius, that is $0.1''$). If the background galaxy has a small gradient in the surface brightness on this scale, the lensing effect is too small to be detectable. This is easily understood: lensing conserves surface brightness, and a uniform source has no lensing effects. This is the case when the lens is far away from the centre of the galaxy. Furthermore, the signal-to-noise (S/N) ratio will be low.

In contrast, near the centre of the galaxy, the surface gradient is high, and so even if the Einstein radius of the lens star is small, the distortion effect at this place can still be strong enough to be detectable. In our simulation, we assume the lens star is close to the centre of the background galaxy. We only use a part of the lensed image which covers 71×71 pixels. With a pixel size of $0.004''$, the area is $0.284'' \times 0.284''$. We assume that within this area, the number of photons from the galaxy is 3.5×10^6 and that from the sky background is 12.5 times higher. The centre of the galaxy is at $(0, 0)$, and the lens is put at $(2.5, -2.5)$ in units of pixel. This position of the lens corresponds to a distance of $0.014''$.

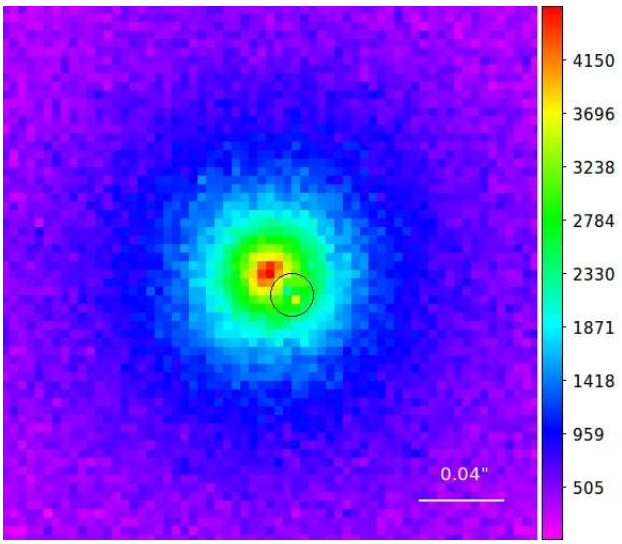

Figure 1. The simulated lensed image by a lens star of Einstein radius $\theta_E = 0.005''$ in the central part of the background galaxy which covers an area of $0.284'' \times 0.284''$. The effective radius of the galaxy is $1''$. The position of the lens is the centre of the circle and the radius of the circle is twice of the Einstein radius. The distance between the lens star and the centre of the galaxy is $0.014''$. Assume the photons from sky background noise is 12.5 times that from the galaxy in this area. The sky background light has been subtracted in this image.

The simulated lensed image is shown in Figure 1. The distortion within the circle in the image is caused by a foreground lens star with an Einstein radius $\theta_E = 0.005''$. The centre of the circle is the position of the lens star and the radius of the circle is $2\theta_E$. In this case, the minimum χ^2 value is 6873. The degree of freedom is $71 \times 71 - (22 \times 22 + 1) = 4556$. Then the reduced minimum effective χ^2 is 1.5. Figure 2 shows the reduced effective χ^2 curve. The best-fit $\theta_E = 0.005^{+0.0003''}_{-0.0002''}$. The 1σ error is derived from the scatters in 300 Monte Carlo realisations. In Monte Carlo realisations, the simulated lensed image d_{ij} are resampled from Poisson distributions. So If there are no errors involved in the estimates of distances of the lens star and the source galaxy, such an error from θ_E ($\sim 6\%$) would translate into an error of $\sim 12\%$ in the mass estimate of the lens star ($\theta_E \propto \sqrt{M}$).

Several factors affect the value of the accuracy of the best-fit θ_E. These are the size of the Einstein radius, the total number of photons and the position of the lens. For comparison, we have repeated our Monte Carlo simulations for several other combinations of parameters. The results are shown in Table 1. In this table, the maximum projected distance between the lens star and the centre of the galaxy is $\sim 0.024''$. It clearly demonstrates that when the Einstein radius increases or the lens is closer to the centre of galaxy (where the gradient in the surface brightness is high), the Einstein radius can be more accurately determined. Furthermore, when the total number of photons increases, the error bar decreases.

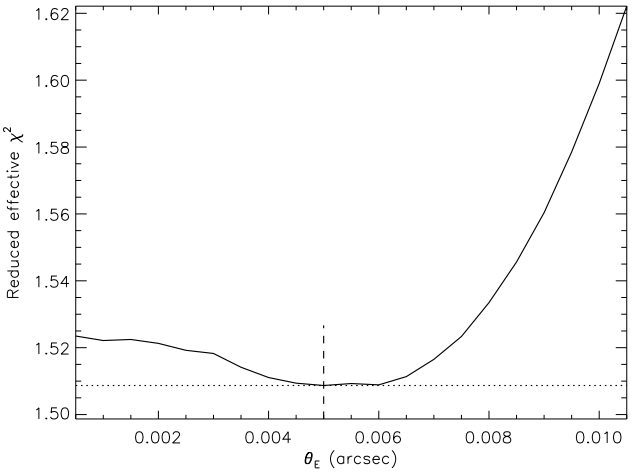

Figure 2. The reduced effective χ^2 for the case shown in Figure 1. The degree of freedom is 4556. The vertical dash line indicates the true Einstein radius $\theta_E = 0.005''$ used in producing the lensed image.

Table 1. 1σ errors for different Einstein radii and lens positions. The distance in the third row is the angular separation between the foreground lens and the centre of the background galaxy. It is in units of the Einstein radius. For each simulation, the total number of photons from the source galaxy (in the considered region) is 3.5×10^6. The photon number from the sky background is 12.5 times higher. θ_E is the true Einstein radius used to produce the lensed images. The 1σ errors are given by Monte Carlo simulations.

θ_E	$0.005''$	$0.005''$	$0.01''$	$0.01''$
lens	(5.5,-2.5)	(2.5,-2.5)	(5.5,-2.5)	(2.5,-2.5)
Distance	4.8	2.8	2.4	1.4
1σ error	$^{+0.0004''}_{-0.0003''}$	$^{+0.0003''}_{-0.0002''}$	$\pm 0.00020''$	$\pm 0.00015''$

4 SEARCHING EXISTING CATALOGUES

We use the known pulsars in the ATNF Pulsar catalogue[2] (Manchester et al. 2005) as our target lens stars. We cross-match this catalogue with several galaxy catalogues, in order to look for existing or promising pulsar-galaxy pairs. An existing pair means that the pulsar is already passing across the surface of the background galaxy while a promising pair means that the pulsar will move across the background galaxy within less than one hundred years. The data sets include

(i) ESO archive data from NACO imaging. The search radius is $1'$. We did not find any pair.

(ii) 2MASS Extended Source Catalog. We found 10 pulsar-galaxy pairs with separation of less than $5''$. Upon closer examination, we find that seven of these belong to the globular cluster 47 Tuc, and two others belong to the globular cluster NGC6544. In these cases, the globular clusters are the "extended" sources rather than galaxies. Only in the single remaining pair, the extended source is a faint galaxy. The information about the promising pair is listed in Table 2.

(iii) the SDSS catalogue [3]. Within a radius of $3''$, there are 4 pairs. The positions of these four pairs are listed in Table 3. The best example is shown in Fig. 3 (the second row in Table 3). The other galaxies in the remaining pairs all have very low signal-to-noise ratios. Further observations are needed to confirm whether they are true galaxies.

We also searched for possible galaxies surrounding the seven thermally emitting radio-quiet isolated neutron stars discovered in the ROSAT all-sky survey (Motch et al. 2009). The galaxy search was limited within the above three databases. Among these, J0420.0-5022 has the closest neighbour galaxy, $\sim 45''$ away from the star. Considering this star has a proper motion of 123 mas/yr (Motch et al. 2009), we have to wait for more than 100 years for the star to move across the galaxy.

4.1 "lensing" probability and integration time

The above search suggests that it is rare that a known pulsar or a neutron star has a close neighbour galaxy or is passing across a background galaxy. Since there will be deeper sky surveys, both in the radio (the Square Kilometer Array [SKA[4]]), and in the optical (e.g. LSST[5], PanSTARRS[6]), it is expected that more and more fainter galaxies and new pulsars will be discovered in the future. Promising pairs can then be observed with diffraction-limited, extremely large optical-IR telescopes.

In this section, we will estimate, with deep imaging, the number of galaxies that can be found in the area of sky swept out by the known pulsars within 10 to 15 years. From Table 1, we see that when the distance is $4.8\theta_E$, we can obtain a best-fit θ_E from one lensed image with one sigma error bar of $\sim 8\%$. In the following, we consider an area affected by a lens star is covered by a diameter of $10\theta_E$. The area swept by each pulsar per year is $\mu \times (10\,\theta_E)$, where μ is the proper motion.

First we estimate the total area for all the pulsars in ATNF catalog[7]. In this catalog, there are 241 pulsars with known proper motions. Among these pulsars, 70% of them has a proper motion within (0, 30) mas/yr. 10 mas/yr is the peak value of the proper motion histogram. We then assume the remaining pulsars without proper motion measurements all have proper motions of 10 mas/yr. With this assumption, the total area swept by the pulsars in ATNF catalog within 15 years by $10\,\theta_E$ is 26.51 arcs^2 for $\theta_E = 0.01''$ and 13.25 arcs^2 for $\theta_E = 0.005''$.

We then use the GalaxyCount program[8] (Ellis & Bland-Hawthorn 2007) to estimate the number of galaxies given the magnitude limit. We convert the K-band number counts to the J-band since there is no J-band option in their program. If TMT can reach

[2] http://www.atnf.csiro.au/people/pulsar/psrcat/

[3] www.sdss.org
[4] www.skatelescope.org
[5] www.lsst.org
[6] http://pan-starrs.ifa.hawaii.edu/public/
[7] The catalog we used was updated on Jul 25, 2012.
[8] http://www.aao.gov.au/astro/GalaxyCount

Table 2. List of one pair found in 2MASS extended Source Catalog cross-matched with the catalogue of Manchester et al. (2005).

Pulsar Name	RA (hms)	Dec (dms)	Galaxy(NED Obj Name)	RA (hms)	Dec (dms)	Separation (arcsecs)	Magnitude (J band)
B1900-06	19:03:37.939	-06:32:21.94	2MASX J19033714-0632191	19:03:37.1	-06:32:19	3.59	13.161

Table 3. List of four pairs found by cross-matching the SDSS catalog and the catalog of Manchester et al. (2005).

Pulsar Name	RA (hms)	Dec (dms)	Galaxy(SDSS obsID)	RA (hms)	Dec (dms)	Separation (arcsecs)	Magnitude (r band)
J0927+23	09:27:37.000	23:46:59.999	587741491435078548	09:27:37.057	23:47:00.675	1.987	22.5
J1238+21	12:38:23.177	21:52:11.075	587742013285794672	12:38:23.203	21:52:11.258	0.414	21.5
J2317+1439	23:17:09.237	14:39:31.219	587730774421078668	23:17:09.230	14:39:31.182	0.104	22.8
B0820+02	08:23:09.768	01:59:12.412	588010358525657901	08:23:09.787	01:59:12.581	0.331	23.2

the magnitude 24.48 in the J-band, and we use a colour $J-K=1.0$ from UKIRT (La Barbera et al. 2010), then we get a magnitude limit of $K=23.48$. The program gives 115 galaxies per sq. arcmin with $K\leqslant 23.48$. For $\theta_E=0.01''$, within the area, 0.85 galaxies will be found. For $\theta_E=0.005''$, the rate is reduced by one half to about 0.42 galaxies.

It is interesting to estimate the required integration time for such a program. The average number of photons is about 15 photons $s^{-1}\,m^{-2}$ at $J=20$ assuming a telescope throughput of about 30%. In Table 4, we list the integration times required for $\gamma_{total}=1.4\times10^8$ for five different magnitudes of the galaxy J=18., 19.496, 20., 20.28, 22. γ_{total} is a total number of photons from the galaxy within the simulated area $0.284''\times0.284''$. At faint magnitudes, the telescope time would become rather prohibitive.

We also investigate the observational feasibilities of the known pairs listed in the tables. We assume the background galaxy has the magnitude 19.50 in the J-band[9] and an effective radius of $1''$, which is similar to the galaxy in the second case in Table 3. For this magnitude, the ratio of the light from the sky background to the galaxy itself within a central area of 0.28×0.28 square arcsecs is 9.0. The distance between the centre of the galaxy and the lens is assumed to be $0.105''$, which is close to the third case in Table 3. With a photon number of 3.5×10^6 from the galaxy in the given central area, the lensing effect for an Einstein radius $\theta_E=0.005''$ is buried in the sky background. But with a higher photon number, such as 1.4×10^8, which corresponds to a S/N ≈ 49 at the lens position, this method can reproduce the input value $\theta_E=0.005''$. However, to collect this number of photons within the given central area of the galaxy, we need about 21 hours for TMT assuming a throughput of 30%.

5 SUMMARY AND DISCUSSION

In this work we studied the feasibility of determining the mass of isolated neutron stars from their lensing effects on background galaxies. When a neutron star is passing in front of a background galaxy, the surface brightness of the background galaxy suffers from distortions. This effect can be used to derive the Einstein radius of the lens if we *assume* there are no intrinsic substructures close to the location of the lens.

Our calculations suggest that once the position of the lens star is identified precisely, the Einstein radius can be derived from only one lensed image of the galaxy given a sufficient number of photons. The Einstein radius can be effectively derived when the background galaxy has a sharp surface brightness gradient near the lens star. We showed that the Einstein radius can be derived with 4-8% accuracy for a size of $0.005''$ if we can achieve the required signal-to-noise ratio. The resulting mass uncertainty is about 8-16%. The main limitation of this method is likely the expensive integration time required, even on extremely large telescopes, from hours to tens of days. This long integration time may be remedied in the future when we have larger pulsar catalogues from SKA, or the overlapping galaxy happens to be bright. Such examples may be already seen (see Table 3 and Fig. 3).

We are being somewhat conservative here by taking just one image. In fact, for a relative proper motion of 10 mas/yr, the pulsar would have moved about 20 mas in two years, five IRIS pixels on TMT and 3 times the point spread function. One can compare the differences in the two images, and thus obtain tighter constraints on the lens mass. We can apply our method to the first-epoch image to infer the lens mass, and then take a second image to further confirm and verify the model.

If the background source is visible in the radio, then an interesting possibility is to observe it with the Square Kilometer Array (SKA). In this case, the resolution can be of the order of milli-arcsecs, and the dynamical range can also be very high. However, one potential problem may be the foreground pulsar will be bright in the radio. Similarly, in the optical, we assumed the neutron star does not contribute any light to the images of the lensed galaxy. However, it may not be the case in reality. Therefore, We need to select the optimal bands to take images of the galaxy in order to minimise the contamination of light from the neutron star.

[9] We use a colour $r-J=1.954$ (La Barbera et al. 2010) for the galaxy. It may have an uncertainty of about 1 mag because we do not know the type of this galaxy.

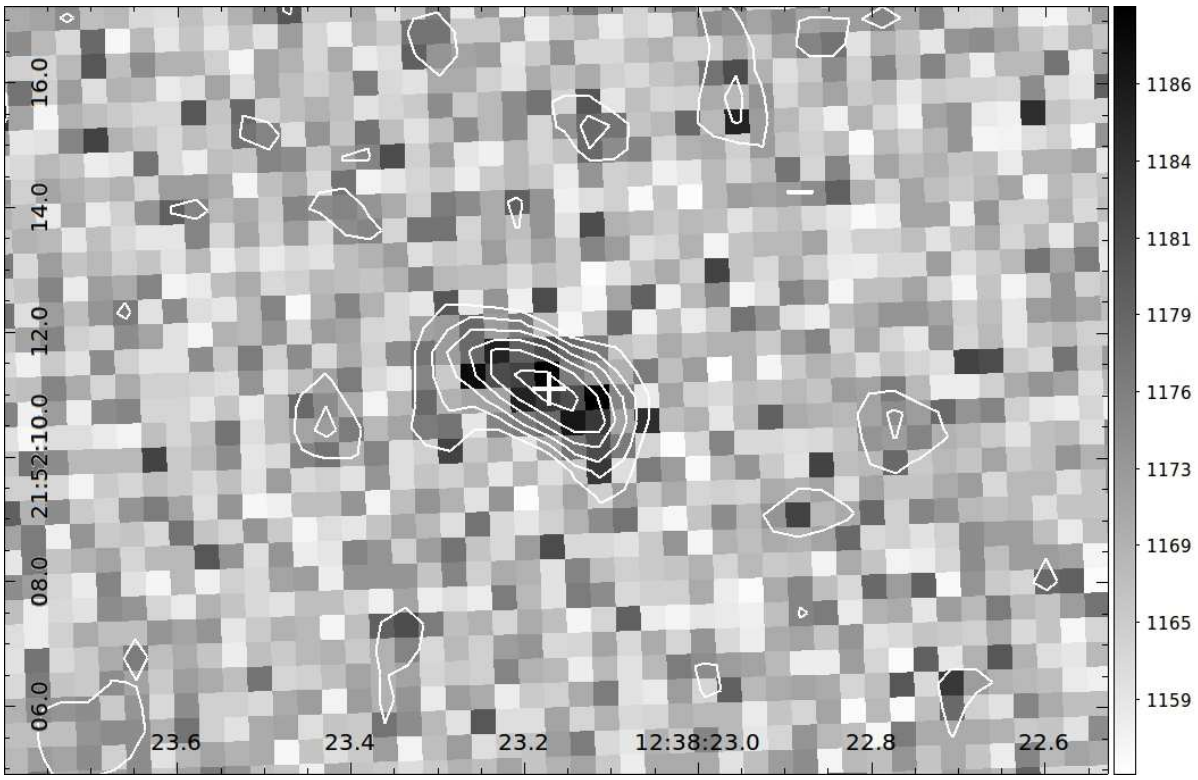

Figure 3. The SDSS image of the galaxy (Obj ID:587742013285794672). Its r-band magnitude is 21.45. At the current time, the pulsar J1238+21 is crossing the surface of the galaxy. The pulsar's position in 1999 (J2000): RA 12:38:23.17, Dec +21:52:11.1. There is no proper motion information available in the literature and no record shows it is a binary system. The white cross indicates the location of the pulsar; the error in the position is about 1 arcsec.

Table 4. Integration time in hours needed to achieve the signal-to-noise ratio for TMT with 30% throughput for $\gamma_{total} = 1.4 \times 10^8$. γ_{total} is a total number of photons from the galaxy within the simulated area $0.28'' \times 0.28''$.

magnitude (J band)	18.	19.496	20.	20.28	22.
Integration time (hours)	5.3	20.8	33.2	42.9	209.02

ACKNOWLEDGMENTS

We thank our referee for his/her helpful comments. We acknowledge the Chinese Academy of Sciences for financial support and Drs. P. Saha, Charles Keeton and Andy Gould for discussions and suggestions. LLT also would like to thank Stephen Justham, Chen Wang and Pengfei Wang for help on pulsar astronomy.

REFERENCES

Arzoumanian, Z., Chernoff, D. F., & Cordes, J. M. 2002, ApJ, 568, 289
Batista, V., Dong, S., Gould, A., et al. 2009, A&A, 508, 467
Coles, J., Saha, P., & Schmid, H. M. 2010, MNRAS, 402, L21
Demorest, P. B., Pennucci, T., Ransom, S. M., Roberts, M. S. E., & Hessels, J. W. T. 2010, Nature, 467, 1081
de Vaucouleurs, G. 1948, Annales d'Astrophysique, 11, 247
Ellis, S. C., & Bland-Hawthorn, J. 2007, MNRAS, 377, 815
Gould, A., Udalski, A., Monard, B., et al. 2009, ApJ, 698, L147
Melchior, P., Meneghetti, M., & Bartelmann, M. 2007, A&A, 463, 1215
Hewett, P. C., Warren, S. J., Leggett, S. K., & Hodgkin, S. T. 2006, MNRAS, 367, 454
Hwang, K. H., Han, C., Bond, I. A., et al. 2010, ApJ, 717, 435
La Barbera, F., de Carvalho, R. R., de La Rosa, I. G., et al. 2010, MNRAS, 408, 1313
Manchester, R. N., Hobbs, G. B., Teoh, A., & Hobbs, M. 2005, AJ, 129, 1993
Mao, S. 2012, Research in Astronomy and Astrophysics, 12, 947
Motch, C., Pires, A. M., Haberl, F., Schwope, A., & Zavlin, V. E. 2009, A&A, 497, 423
Paczynski, B. 1995, Acta. Astronom., 45, 345
Posselt, B., Neuhäuser, R., & Haberl, F. 2009, A&A, 496, 533
Refregier, A. 2003, MNRAS, 338, 35
Sánchez, S. F., Thiele, U., Aceituno, J., et al. 2008, PASP,

120, 1244
Smith, M. C., Mao, S., & Woźniak, P. 2003, ApJ, 585, L65